Spatiotemporal Dynamics of Quantum Computing Dipole-Dipole Block Systems

Hideaki Matsueda
Department of Information Science, Kochi University
2-5-1 Akebono-cho, Kochi 780-8072, Japan
e-mail: matsueda@is.kochi-u.ac.jp

November 18, 2018

Abstract

The stability of dynamic dipole-dipole interactions in a quantum dot array is estimated, and a novel solid state quantum CCN (controlled controlled not) gate having a block structure of quantum dot array is proposed. Quantum mechanical coherence is expected to be maintained, and both the bit error and the phase error are reduced by the ensemble effects in the block. The overall process of quantum computing is presented schematically, showing four main steps. The spatiotemporal dynamics of the quantum entangled pure state, which is the kernel of the quantum super-parallel computation, is also illustrated for the proposed quantum CCN gate.

1 Introduction

We have been proposing solid state quantum gates, employing a coherent mode induced by the dynamic dipole-dipole interaction among ensemble of Frenkel type excitons, each of which being confined in a three dimensional quantum dot, see Appendix A [1][2][3].

Our treatment of the dipole-dipole interaction is different from previous ones [4][5], in that we employed the dynamic dipole-dipole interaction to enhance the coherence, whereas static dipole-dipole interaction is used just to execute particular logic in the case of ref.[5]. In the next section (x2) of this paper, the stability of this dynamic dipole-dipole interaction is estimated energetically.

A pair of the block is expected to constitute a realistic solid state quantum CN (controlled not) gate, having extra coherence due to the dynamic dipole-dipole interactions, and also due to cancellation of phase fluctuation in the ensemble of quantum dots [1]. Then it may be possible to construct universal quantum systems, employing this CN gates and few other kinds of simple gates. In this way, a quantum CCN (controlled controlled not) gate is proposed as an essential part of the universal system for quantum computation.

The overall process of quantum computing is analyzed schematically, showing four main steps, i.e. preparation and input, arithmetic procedure entangling different bits, interfering procedure to reduce the uncertainty (i.e. collapse of wave function), and the final output. The spatiotemporal dynamics of the quantum entangled pure state, which is the kernel of the quantum super-parallel computation, is illustrated for the proposed quantum CCN gate of logical block structure.

2 Energetics of the Dipole-Dipole Interaction in the Block

2.1 Dipole-Dipole Energy

The array of dipole moments p_m arranged at positions R_m impose a resultant electric field $E(n)$ on a site at R_n as given below for $n \neq m$.

$$E(n) = \frac{1}{4\pi\varepsilon_0} \sum_m \frac{p_m}{|R_n - R_m|^3} - 3\frac{p_m \cdot (R_n - R_m)(R_n - R_m)}{|R_n - R_m|^5} \tag{2.1}$$

in SI unit. Then the average energy Q of the total dynamic dipole-dipole interaction in a block per single quantum dot may be given as

$$Q = \frac{1}{N} \sum_n p_n \cdot E(n) \tag{2.2}$$

where N is the total number of quantum dots in the block being larger than the overall number of excitons in it, and in the summation double counting of the same quantum dot pair should be avoided, because the dynamic dipole-dipole induction occures between a quantum dot having an exciton and another dot having no exciton initially [1].

The dipole-dipole energy of eq.(2.2) is plotted as a function of the separation of quantum dots in Fig.1, for the array having identical dipole moments all directed along z

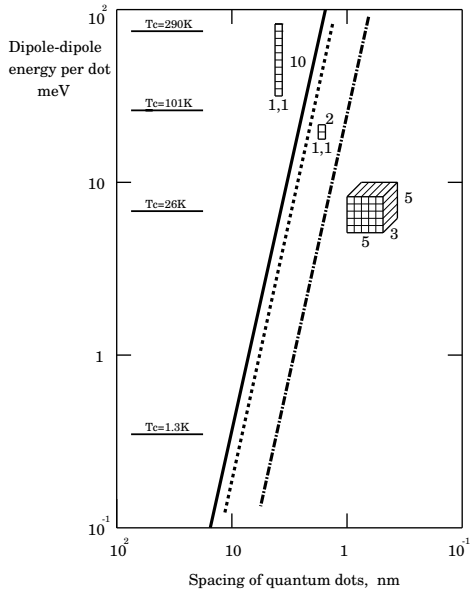

Figure 1: Dipole-dipole interaction energy per quantum dot as the function of the spacings of quantum dots, for different block dimensions 1–1–10 (solid), 1–1–2 (dotted), and 5–3–5 (dot-dash). The Curie temperature (T_C) for the dipole-dipole energy 75.0, 26.1, 6.8, and 0.35 meV are also indicated. The dipole length is assumed to be 0.35nm as in GaAs.

direction, which is the result of the initial optical excitation. The dipole moment is assumed to be, as an example, that of GaAs; $p = |p| = ed = 3.5 \times 10^{-10}$ emC [6], with elementary electric charge $e = 1.60219 \times 10^{-19}$ C $= 4.80321 \times 10^{-10}$ esu. The plotting is done for three kinds of blocks, of which dimensions (x, y, z) are (1, 1, 10), (1, 1, 2) and (5, 3, 5) [2].

As is explained in detail elsewhere [1], including this dynamic dipole-dipole energy in the starting Hamiltonian (using eq.(A.6) in xA), we derived a collective localized coherent mode below a conventional excitonic band, in a regime where the population difference is below a critical value, which is estimated to be for an example 0.87 (corresponding to 94% excitation) in the case of 2.6nm spacing GaAs quantum dots. In this model, the confinement of the exciton is assumed to be so perfect, that no considerable overlapping of wave function and no tunneling among them are expected. This localized mode may be useful as the excited state of a quantum gate, because of its ferromagnetic type stability.

2.2 Curie Temperature

The field of eq.(2.1) could be thought of as the molecular (or Weiss) field in ferromagnetic materials, although usually static field is considered as the molecular field the induced field of this equation is dynamic [1][3][7]. For a three dimensional array of identical dipoles of which polarizations are all directed along the z direction, the molecular field is given as $jE(n)j = N p$, and the Curie-Weiss law $= \frac{C}{T \; T_c}$ may be reasonable for the susceptibility , with a Curie constant $C = \frac{N p^2}{3k}$, the Curie temperature $T_c = C$, and the Boltzmann constant k, following the procedure of ferromagnetism [7]. The Weiss constant is evaluated using eqs.(2.1) and (2.2) to give

$$T_c = \frac{Q}{3k}: \tag{2.3}$$

Typical values of T_c, i.e. 290, 101, 26, and 1.3K are given in Fig.1 for the dipole-dipole energies 75.0, 26.1, 6.8, and 0.35meV respectively.

2.3 Ensemble Stability

It is seen from Fig.1 that the block having the minimum dimension in x-y plane has the largest dipole-dipole energy, ex. (1, 1, 10) block which is an one dimensional array with 10 quantum dots along the z direction. In this case, the parallel (ferromagnetic type) phase is stable even at room temperature if the quantum dot spacing is less than 1.7nm , and it is stable at 77K and 4K if the spacing is below 2.6nm and 7.1nm respectively. In the (5, 3, 5) block having 5 3 two dimensional arry in x-y plane and 5 layers along the z direction, it is stable at 77K and 4K if the spacing is less than 1nm and 2.8nm respectively.

The stability increases if we employ materials with larger dipole moments; for example in the case of InSb of which dipole moment is approximately 7 times larger than that of GaAs [6], the dipole-dipole energy is larger by a factor of about 50, resulting in the room temperature T_c at separation of 6.2nm in (1, 1, 10) block, and at 2.5nm in (5, 3, 5) block. This might improve further if some organic materials with gigantic dipole moments are used.

It is also obvious that in this block accommodating the dynamic dipole-dipole interaction, the stability does not directly depend on the volume of the block or the number of dipoles, although that may be the case in other kinds of memory devices [8]. In our case, the more the side-by-side dipole arrangement, the less the total dipole-dipole energy gain within the block, because a dipole moment produces a field in the antiparallel direction

at the side-by-side positions. Therefore, the stability depends on the shape (internal configuration) of the block rather than the volume of it. As a matter of course, our method of calculation based on eqs. (2.1) and (2.2) takes care of the depolarization fields from the surfaces.

The coupling between the dipole moment of the block and dipole moments in the environment, should be minimized by surrounding the devise by vacuum or materials of very small dielectric constants. Numerical estimation similar to that of Fig.1 shows that vacuum spacing of 500 m is sufficient to suppress the environmental dipole-dipole coupling below 10^{-11} meV per dot in a (1, 1, 10) block, assuming as the environment an (1, 1, 10) array of 10 dipoles each moment of which is 100 times larger than GaAs.

Furthermore, the spontaneous emission rate should also be considerably controlled, by some cavity type structure [10] designed to have a photonic band gap wide enough to cover the wavelength range of importance. Moreover, some structure creating phononic (acoustic) band gap [11] may also be useful to avoid the coupling of quantum bits to lattice vibrations. These may further help suppress dissipative decohering.

3 Resistance of the Quantum Logical Blocks to Bit and Phase Errors

3.1 Bit Error Resistance

There is a whole bunch of energy levels arising from all the quantum dots in the same block, including energetically degenerate states. Superposition (or intra-block entanglements) of states having same multiple number n of excited sites may be generated dynamically in a block having total N quantum dots, by an appropriately precision pulse.

This state

$$\sqrt{\frac{n!(N-n)!}{N!}}\;|1,1,\ldots,1,0,0,\ldots,0\rangle + |0,1,1,\ldots,1,0,\ldots,0\rangle + |0,0,1,1,\ldots,1,0,\ldots,0\rangle + \cdots \Longrightarrow |\Psi\rangle \tag{3.1}$$

and the physical ground state

$$|0,0,0,\ldots,0\rangle = |0\rangle_{ij} \tag{3.2}$$

should work as a dual basis ($|\tilde{0}\rangle$, $|\tilde{1}\rangle$) for the computation. Thanks to the dynamic dipole-dipole interaction, it is natural from the results of previous section (x2) to expect the resistance (immunity) of these basis states to thermal agitations, preserving the basic coherence for the quantum computation. First of all, this interaction is obviously helpful to prevent bit errors (amplitude errors) such as $|0\rangle \to |1\rangle$ and $|1\rangle \to |0\rangle$. Moreover, this could also be effective to avoid phase errors as explained in the next subsection (x3.2).

3.2 Phase Error Resistance

It may be possible to generate another orthogonal basis ($|\tilde{0}\rangle$, $|\tilde{1}\rangle$) by an Hadamard transformation

$$H = \frac{1}{\sqrt{2}} \begin{pmatrix} 1 & 1 \\ 1 & -1 \end{pmatrix} \tag{3.3}$$

as

$$H|0\rangle = \frac{1}{\sqrt{2}}(|0\rangle + |1\rangle) \Rightarrow |\tilde{0}\rangle \tag{3.4}$$

$$H|1\rangle = \frac{1}{\sqrt{2}}(|0\rangle - |1\rangle) \Rightarrow |\tilde{1}\rangle, \tag{3.5}$$

which is easily derived by substitution $|0\rangle = \begin{pmatrix} 1 \\ 0 \end{pmatrix}$ and $|1\rangle = \begin{pmatrix} 0 \\ 1 \end{pmatrix}$.

This transformation increases the resistance of the coding against phase errors, because a phase error in ($|\tilde{0}\rangle$, $|\tilde{1}\rangle$) basis corresponds to a bit error in the ($|0\rangle$, $|1\rangle$) basis, as is easily seen from the transformation in eqs.(3.4) and (3.5), for the case of phase error such as $|\tilde{0}\rangle \to |\tilde{0}\rangle$ and $|\tilde{1}\rangle \to -|\tilde{1}\rangle$, of which consideration may be sufficient for our purpose [12].

There is also cancellation of phase fluctuations in the quantum dot ensemble. The phase fluctuations of an off-diagonal element of the density matrix in the ($|0\rangle$, $|1\rangle$) basis or even in the ($|\tilde{0}\rangle$, $|\tilde{1}\rangle$) basis, should cancel each other, as the number of excited site n increases. This saves the off-diagonal terms in the ensemble, supporting the generation of entanglements in a block surrounded by the environment.

The situation is easily seen in the bosonic heat bath model, where the phase fluctuations of the excited state and the ground state both at site k may be represented as $_k$ and $_k$ respectively, and their distributions are Gaussian having their means at zero [13].

The total phase fluctuation may be expressed as

$$\begin{aligned} \delta_i &= (\delta_1 + \delta_2 + \cdots + \delta_{k-1}) + (\delta_k + \delta_{k+1} + \cdots + \delta_{k+n-1}) \\ &\quad (\delta_{k+n} + \delta_{k+n+1} + \cdots + \delta_N) \\ &\to 0 \quad \text{for } n, N \to 1 ; \end{aligned} \tag{3.6}$$

for a state i, leading to

$$\begin{aligned} & e^{i\delta} |0;0 \cdots 0;1;1 \cdots 1;0;0 \cdots i\rangle \\ &= e^{i\delta_1} |0_1 i \cdots e^{i\delta_k} |1_k i \cdots e^{i\delta_{k+n}} |0_{k+n} i \\ &= e^{i(\delta_1 + \delta_2 + \cdots + \delta_{k-1}) + (\delta_k + \delta_{k+1} + \cdots + \delta_{k+n-1}) (\delta_{k+n} + \delta_{k+n+1} + \cdots + \delta_N)} \\ &\qquad |0;0 \cdots 0;1;1 \cdots 1;0;0 \cdots i\rangle \\ &\to |0;0 \cdots 0;1;1 \cdots 1;0;0 \cdots i\rangle \end{aligned} \tag{3.7}$$

Such cancellation may be carried on further by the summation of the degenerate states within the computational basis given by eq.(3.1). These may be considered as the ensemble cancellation of random phase fluctuation. As a matter of course, the possible numbers of quantum dots N and the excited sites n are limited by technological conditions, leaving a finite phase fluctuation for δ_i of eq.(3.6). There should be an optimum condition for the numbers N and n, and the permissibility of errors in each practical computation.

3.3 Error Prevention Methods

Two methods to avoid the phase decoherence of encoded states during some significantly complex computation are considered.

One is a divide and conquer strategy, dividing the total computational algorithm into shorter pieces, in such a way that each piece could be executed by a small scale block structure. If we denote the statistical variance of the temporal phase fluctuation in each identical quantum dot as σ^2, then the ensemble average in ith block consisting of N_i quantum dots gives variance $\frac{\sigma^2}{N_i}$. Therefore the whole computing structure of M blocks may suffer from $\sum_{i=1}^{M} \frac{\sigma^2}{N_i}$, which corresponds to a standard deviation on the order of $\sqrt{\frac{M}{N}}\,\sigma$.

However, this deviation remains finite, so long as each piece of the algorithm (eventually M) is sufficiently small. The optimum value of $\frac{M}{N}$ depends on how successfully the algorithm could be devided, as well as the error correction scheme and the required accuracy of computation.

The other method is to execute the phase sensitive part of the computation in the $(|\tilde{0}\rangle, |\tilde{1}\rangle)$ basis given by eqs.(3.4) and (3.5). In this basis, the phase error is suppressed directly by the dynamic dipole-dipole interaction among the ensemble of quantun dots in each block, as discussed in x3.1 and x3.2. As a matter of course, some gates or operations should be added at the beginning of such processes as in the fields B^0 and C^0 of Fig.2 in next subsection (x4.1), to practice the transformation of eqs.(3.4) and (3.5) between the bases.

4 Quantum Computing Systems

It is possible to construct quantum computing systems out of the blocks given in previous section (x2). Each block works as a bit for computation (qubit), being represented by a small box in Fig.2. Every row in Fig.2 corresponds to a physical row of the blocks.

4.1 Overall Quantum Computing Process

An architectural representation of a solid state qunatum computer, consisting of the input port (A), first computing field (B), second computing field (C), and output port (D) is given in Fig.2. The overall process of quantum computation may be understood as comprising four main steps corresponding to fields A, B, C and D. Fig.2 could also represent this common situation schematically, for quantum computers of different methods such as ion trap [14][15], CQED (cavity quantum electrodynamics) [16], and NMR (nuclear magnetic resonance) [17][18], besides the solid state method [2]. Each row represents a quantum state, which evolves from row to row to the final solution state through row operations.

The first step is to prepare the preparation registers (section A), making a superposition (minimum entanglement) of the ground state $|0\rangle$ and the excited state $|1\rangle$ in each bit in the preparation register 1, and a ground state in each bit in the preparation register 2. The latter preparation register is used to accomodate intermediate results in some algorithms such as for factoring [19]. The initial preparation state is the state of maximum intrinsic uncertainty in the first preparation register 1 [20].

Computation proceeds as the downward sequential execution of the elemental row operation, which is the unitary (or quasiunitary) evolution driven by the propagation of the excited states into the fields initially kept at the ground states [2]. A consecutive activation of the row of blocks is assumed, employing methods of clock signal and biased

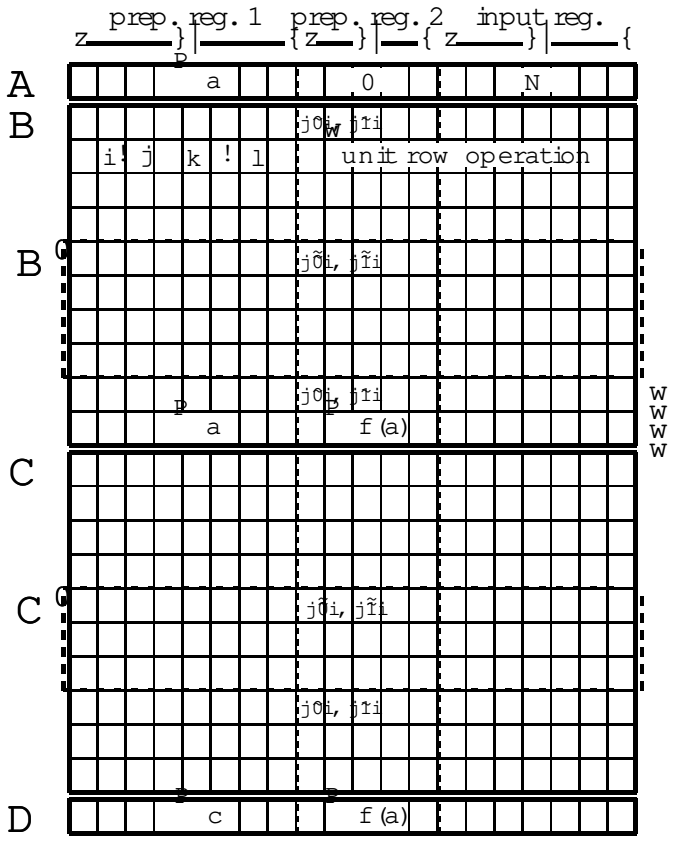

Figure 2: A schematic diagram representing sequential steps in quantum computing. Field A is the input port, providing the preparation registers 1 and 2 on the left, and the input register on the right. Field B is the first bank of row operations containing the arithmetic algorithim for the super-parallel quantum computation. Field C is the bank of row operations such as quantum Fourier transform designed to reduce overall intrinsic uncertainty, and Field D is the output port. Fields B and C might contain subsections B' and C' for reducing phase errors.

band gap explained in x4.2 [2]. Each elemental row operation includes numbers of unit operations among the different bits, such as CN, CR (controlled rotation), and CPS (controlled phase shift), as indicated by $i \to j$ and $k \to l$ (i,k control bits, j,l target bits). In each elemental row operation, every unit operation is executed just once in parallel. The temporal nature of this pairwise logical relation may be visualized by a diagram in a state space, as demonstrated elsewhere [20].

In the second step, sequential execution of a bank of row operations proceeds in field B. This is the unitary evolution, generating the quantum mechanical entangled pure states [21]. This is a spontaneous process resulting in a superposition of different product states involving different bits. A row operation may increase or decrease the intrinsic uncertainty

(dispersion) of the preceding state [20].

The third step is another unitary evolution, converging into the final less dispersive states, or even into the dispersion-free pure state. This is achieved as the cumulative effects of rotary operations causing interference among the quantum bits. Thus, the intrinsic uncertainty will be minimized or even extinguished at the stage of the final solution, in the output port such as D of Fig.2. For example, the quantum Fourier transform in the factoring algorithm [13][19][24][25] corresponds to this step in the field C of Fig.2 [26]. The iterative combination of two Walsh-Hadamard transforms and a CPS (or conditional phase shift) in a quantum search algorithm [27], and the building up the correlation function in a quantum simulator [28] may also be considered as this third step.

The computational dual basis is switched into another orthogonal basis ($|\tilde{0}\rangle$, $|\tilde{1}\rangle$) by an Hadamard transformation as described in x3.2, at the beginning of the fields B' and C' where stronger phase error resistance is requiered.

The fourth step, which we represent as field D in Fig.2, is the reading or measuring of the final solution state. The less the uncertainty in this final state, the more accurately one can read it [20]. The result may be read by photonic probing which involves auxiliary higher energy states [1][2].

4.2 Cotrolled Controlled Not Unit

As a simple example, a detailed structure of a CCN gate is given in Fig.3, which consists of two CN, three CR, and two CPS gates, beeing an essential structure to execute Boolean algebra for universal quantum computing systems.

Each line of bit a, b, consists of blocks a_1, a_2, b_1, b_2, . The separation of quantum dots is better to be designed to differ line by line, to distinguish individual line from each other photonically [2]. A CN operation $\hat{P}_{CN}$ is implemented by the couple of blocks facing each other (i.e. a_3 and b_3, a_5 and b_5) and a photonic pulse. Rotational operations $\hat{R}^{=2}$ and $\hat{R}^{3=2} = \hat{R}^{=2}$ are also implemented by the couples of blocks (i.e. b_2 and c_2, b_4 and c_4, and a_6 and c_6) and a photonic $\frac{}{2}$ pulse and a $\frac{3}{2}$ pulse respectively. The phase difference between lines a, b and line c is adjusted by a pair of controlled phase shifters ($\hat{S}^{\frac{}{2}}_{ab}$ and $\hat{S}^{\frac{}{2}}_{ba}$).

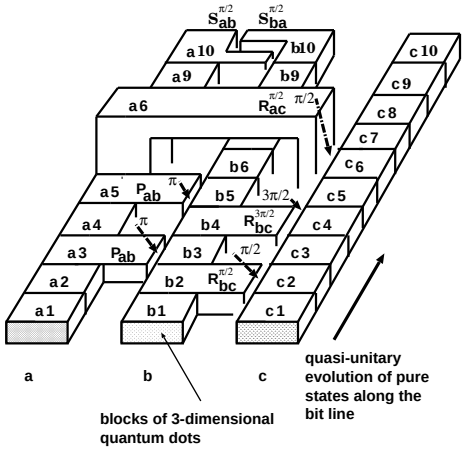

Figure 3: A solid block CCN gate, combining two CN gates (P_{ab}), two $\frac{}{2}$ controlled rotators ($R_{bc}^{=2}$ and $R_{ac}^{=2}$), one $\frac{3}{2}$ controlled rotator ($R_{bc}^{3=2}$), and a pair of $\frac{}{2}$ controlled phase shifters ($S_{ab}^{\frac{}{2}}$ and $S_{ba}^{\frac{}{2}}$). Arrows with , $\frac{}{2}$, and $\frac{3}{2}$ denote the respective photonic pulses.

The CCN operation of Fig.3 may be described as

$$\hat{P}_{CCN} = \hat{S}_{ba}^{\frac{}{2}}\hat{S}_{ab}^{\frac{}{2}}\hat{R}_{ac}^{=2}\hat{P}_{CN\,ab}\hat{R}_{bc}^{3=2}\hat{P}_{CN\,ab}\hat{R}_{bc}^{=2} \tag{4.1}$$

$$= \hat{S}_{ba}^{\frac{}{2}}\hat{S}_{ab}^{\frac{}{2}}\left(1+\frac{1}{4}(1+{}_a^z)(1+{}_b^z)(1-{}_c^x)\right); \tag{4.2}$$

with $\hat{R}^{=2} = \begin{pmatrix} 1 & i \\ i & 1 \end{pmatrix}$; where ^{x}, ^{y}, ^{z} are the Pauli operators, and and correspond to each other [29].

The non-Boolean superposed state such as $\frac{1}{\sqrt{2}}(|0\rangle + |1\rangle)$ may be generated initially by a photonic $\frac{}{2}$ pulse bit by bit, and then conveyed from one block to the other, across different bit lines through the gates such as CN and CR, as well as propagated within the same bit line. After an appropriate time period, an expected entangled pure state (spontaneously generated superposition of different product states involving different bit lines) is attained, being specific to the arrangement of the blocks.

It is helpful if the depth and/or width of the quantum dots could be implemented to cause a small but sequential decrease of the energy gap, starting from the input port toward the output port, block by block along each bit line. Excitons generating the dipole moments may be transferred in one-way fashion through this biased path, bacause there

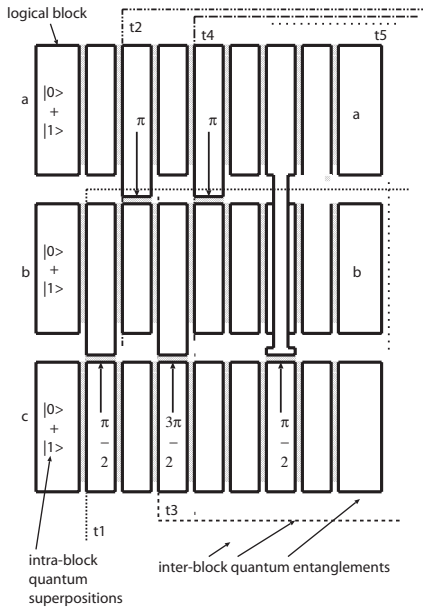

Figure 4: Spatiotemporal dynamics of quantum entangled pure states in the quantum CCN gate of quantum logical blocks. The basins of 5 entangled pure states generated at 5 different times $t_1, t_2,$ are indicated by the dotted or dot-dash lines.

exists some dissipative energy loss which deprives the excitons of their energy to climb back the line. Application of microwave pulses with proper energy may work as clock signals. These methods are expected to facilitate the directional quasi-unitary evolution of the whole system that is needed and sufficient for the quantum computation.

5 Generation of the Quantum Entangled Pure State and its Spontaneous Accumulation into the Output Port

The spatiotemporal dynamics of the quantum entangled pure states is essential for the quantum super-parallel computation. In the quantum CCN gate of Fig.3, it is possible to define a basin for each quantum entanglement generated at a CN gate or at a controlled rotator, as indicated in Fig.4 by dotted or dot-dash lines on the top view of the CCN gate, labeling by the times of generation $t_1, t_2,$, and t_3. The basin may be thought of as the area that is going to be influenced by a gate starting each entanglement.

All the necessary Boolean algebra are executed by inter-block operations, whereas the

purely quantum mechanical superposition and interference of different states will take place in an intra-block manner (within each block). Nonetheless, the quantum interplay of different blocks will be spontaneously realized as the inter-block entanglement via Coulombic interaction, on the way of the unitary (or quasi-unitary) evolution [21]. Then, blocks become incompatible each other, revealing the peculiarity of quantum mechanics. It is no longer possible to measure the states of individual blocks simultaneously, without destroying the states as they are, unless the whole thing settle down in the output port to yield the computational result without any significant uncertainty that causes collapse of the pure state wave function. The temporal evolution of logical states during this process may also be visualized diagramatically as presented elsewhere [20].

The resultant final state is best to be designed to form a pattern of electron excitation with sharply localized peaks at particular blocks in the output port, as the results of the interference of wave functions (or the probability amplitudes), which may be achieved by rotational operations embeded in the algorithms such as quantum Fourier transforms [26], as discussed in §4.1. Therefore this result should be read by a kind of photonic probing, involving some auxiliary higher energy states [1][2].

6 Concluding Remarks

The ferromagnetic type ensemble of dipole moments induced by the dynamic dipole-dipole interaction could suppress not only bit errors in the $(|0\rangle, |1\rangle)$ basis, but also phase errors in $(|\tilde{0}\rangle, |\tilde{1}\rangle)$ basis. Furthermore, the ensemble cancellation of the phase fluctuation in the block is also expected to improve the phase coherence for the quantum computation.

A quantum CCN gate is proposed as the essential element of the solid state quantum computing system, employing the logical blocks of three dimensional quantum dot array which sustains the dynamic dipole-dipole ensemble.

The overall process of quantum computing is presented schematically, showing four main steps. The spatiotemporal dynamics of the quantum entangled pure state, which is the kernel of the quantum super-parallel computation, is also illustrated for the proposed quantum CCN gate of logical block structure.

It is needless to mention that significant technological development is expected, for example precision fabrication of quantum dot array blocks either of semiconductor or other materials including organic compounds, in order to implement the proposed quantum systems for practical computation. Focused photonic pulse technique should also be

developed, for an example the scanning near-field method, for the input superposition and the logical and rotational operations.

Acknowledgments
This work is partially supported by the Proposal-Based New Industry Creative Type Technology R&D Promotion Program of the New Energy and Industrial Technology Development Organization (NEDO) of Japan.

References

[1] H. Matsueda, and S. Takeno, IEICE Trans. Fundamentals Electron., Commun. and Computer Sci., E79-A, 1707 (1996); E80-A, 1610 (1997); in Proc. 1st. Int. Conf. on the Theory and Appl. of Cryptology (Pragocrypt'96), ed. J. Pribyl (GC UCMP, Praha, 1996) pp.225{233; in Proc. 4th Workshop on Physics and Computation (PhysComp96), eds. T. Toffoli, M. Biafore and J. Leao (New England Complex Systems Institute, Cambridge, Massachusetts, 1996) pp.215{222; H. Matsueda, Superlattices and Microstructures, 24, 423 (1998).

[2] H. Matsueda, in Proc. The European Conference on Circuit Theory and Design (ECCTD'97), Budapest (30 Aug. { 3 Sept., 1997) pp.265-270 (invited paper for the special session "Towards Nanoelectronics"); in Unconventional Models of Computation, eds. C. S. Calude, J. Casti, and M. J. Dinneen (DMTCS Series, Springer-Verlag, Singapor, 1998) pp.286-292; in Proc. 1998 SPIE Photonic Quantum Computing II, at AeroSense'98, (Orlando, SPIE { Society of Photo-Optical Instrumentation Engineers, 1998), SPIE Proc. vol.3385 (1998) pp.84-94; in Proc. The First NASA International Conference on Quantum Computing and Quantum Communications (NASA-QCQC'98), (Lecture Notes in Computer Science, Springer-Verlag 1999).

[3] Claude Cohen-Tannoudji, Bernard Diu, and Franck Laloe, Quantum Mechanics (John Wiley & Sons, New York, 1977) Chap.11.

[4] G. Mahler and V. A. Weberruß, Quantum Networks (Springer Verlag, Berlin, 1995), Sec. 2.4.2.1; W. G. Teich, K. Obermayer, and G. Mahler, Phys. Rev., B 37, 8111 (1988); W. G. Teich and G. Mahler, Phys. Rev., A 45, 3300 (1992).

[5] A. Barenco, D. Deutsch, and A. Ekert, Phys. Rev. Lett., 74, 4083 (1995).

[6] M. Asada and Y. Suematsu, IEEE J. Quantum Electron., QE-21, 434 (1985).

[7] C. Kittel, Introduction to Solid State Physics 4th ed. (John Wiley, 1971) Chaps. 13 and 16.

[8] J.A. Swanson, IBM J., (July, 1960) p.305.

[9] H. Matsueda, IEICE Trans. Fundamentals Electron., Commun. and Computer Sci., E82-A, 658 (1999).

[10] M. Bayer, T. Gutbrod, J.P. Reithmaier, and A. Forchel, Phys. Rev. Lett. 81, 2582 (1998).

[11] J.V. Sanchez-Perez, D. Caballero, R. Martinez-Sala, C. Rubio, J. Sanchez-Dehesa, F. Meseguer, J. Llinares, and F. Galvez, Phys. Rev. Lett., 80, 5325 (1998).

[12] A.M. Steane, Phys. Rev., A 54, 4741 (1996).

[13] A. Barenco, A. Ekert, K.-A. Suominen, and P. Torma, Phys. Rev., A 54, 139 (1996); ibid. 147.

[14] S.R. Jeffers, C. Monroe, E.W. Bell, and D.J. Wineland, Phys. Rev. A 51, 3112 (1995); C. Monroe, D.M. Meekhof, B.E. King, W.M. Itano, and D.J. Wineland, Phys. Rev. Lett. 75, 4714 (1995).

[15] J. I. Cirac and P. Zoller, Phys. Rev. Lett. 74, 4091 (1995); T. Sleator and H. Weinfurter, Phys. Rev. Lett. 74, 4087 (1995); M. Reck, A. Zeilinger, H.J. Bernstein, and P. Bertani, Phys. Rev. Lett. 73, 44 (1994).

[16] Q.A. Turchette, C.J. Hood, W. Lange, H. Mabuchi, and H.J. Kimble, Phys. Rev. Lett. 75, 4710 (1995).

[17] D.G. Cory and T.F. Havel, in Proc. 4th Workshop on Physics and Computation (PhysComp96), eds. T. Toffoli, M. Biafore and J. Leao (New England Complex Systems Institute, Cambridge, Massachusetts, 1996) pp.87-91.

[18] N.A. Gershenfeld and I.L. Chuang, Science 275, 350 (1997).

[19] D.R. Simon, in Proc. of the 35th Annual Symp. on the Foundations of Computer Science (FOCS), ed. S. Goldwasser (IEEE Computer Society Press, Los Alamitos, 1994), pp.116{123; P.W. Shor, ibid. pp.124{134.

[20] H. Matsueda and D. W. Cohen, Int. J. Theor. Phys., 38, 701 (1999); A theoretical framework is developed to evaluate the amount of intrinsic uncertainty, as distinguished from operational uncertainty (noises) inherent in quantum computation. The temporal evolution of states in quantum computing is analized diagramatically, providing a visual tool for the refining of quantum algorithms to help achieve minimal uncertainty and maximal efficiency, as well as for better understanding of the quantum entanglements crucial to quantum computing.

[21] We are assuming pure state entanglement as the idealistic case for simplicity, however it may be interesting to include mixed states which leads to mixed state entanglement or even bound entanglement [22][23]; H. Matsueda, in preparation to Phys. Rev. A (1999).

[22] M. Horodecki, P. Horodecki, and R. Horodecki, Phys. Rev. Lett., 80, 5239 (1998).

[23] C. H. Bennett, D. P. DiVincenzo, J. A. Smolin, and W. K. Wootters, Phys. Rev. A. 54, 3824 (1996); D. P. DiVincenzo, T. Mor, P. W. Shor, J. A. Smolin, and B. M. Terhal, quant-ph/9808030.

[24] C. Miquel, J. P. Paz, and R. Perazzo, Phys. Rev. A 54, 2605 (1996).

[25] D. Beckman, A. N. Chari, S. Devabhaktuni, and J. Preskill, Phys. Rev. A 54, 1034 (1996).

[26] This interference process may be accompanied with a partial collapse of pure state wavefunction, which could be called as dis-entanglement in algorithms such as the factoring [19]; as mentioned in A. Peres, Superlattices and Microstructures, 23, 373 (1998).

[27] L. K. Grover, Phys. Rev. Lett. 79, 325 (1997).

[28] S. Lloyd, Science 273, 1073 (1996).

[29] A. Barenco, C. H. Bennett, R. Cleve, D. P. DiVincenzo, N. Margolus, P. Shor, T. Sleator, J. A. Smolin, and H. Weinfurter, Phys. Rev. A 52, 3457 (1995).

A Quantum mechanical consideration of the nonlinear localized coherent mode due to the dynamic dipole-dipole interaction in an ensemble

The atomic Hamiltonian and the eigen vectors for a couple of two level systems each confined in three dimensional quantum dots at sites i and j may be expressed as

$$H_0 = H_{0i} + H_{0j} \tag{A.1}$$

$$|\ _1\rangle = |1_i\rangle + |0_j\rangle; \quad |\ _r\rangle = |0_i\rangle + |1_j\rangle: \tag{A.2}$$

Assuming a degenerated pair having no overlappings of wave functions,

$$\begin{aligned} \langle\ _1|H_0|\ _1\rangle &= \langle\ _r|H_0|\ _r\rangle \\ &= \langle 1_i|H_{0i}|1_i\rangle + \langle 0_j|H_{0j}|0_j\rangle \\ &= \langle 0_i|H_{0i}|0_i\rangle + \langle 1_j|H_{0j}|1_j\rangle \\ &= E_0: \end{aligned} \tag{A.3}$$

Now, an interaction Hamiltonian H_I for the dynamic dipole-dipole interaction H_{dd} is included as

$$H = H_0 + H_I \tag{A.4}$$

$$= H_{0i} + H_{0j} + H_{dd} \tag{A.5}$$

where the orbital and magnetic quantum numbers, and higher order interactions are neglected for simplicity.

For the dynamic dipole-dipole induction between sites i and j,

$$H_{dd}(i,j) = \frac{1}{4\ _0}\ \frac{p_i\ \ p_j}{|R_i\ \ R_j|^3}\ \ 3\frac{p_i\ \ (R_i\ \ R_j)\ p_j\ \ (R_i\ \ R_j)}{|R_i\ \ R_j|^5} \tag{A.6}$$

where p_i and R_i are the electric dipole momoment vector and the position vector respectively, at site i. This situation is analogous to the resonance dipole-dipole interaction between a couple of hydrogen atoms, one is in 1s state and the other in 2p state [3]. The

interaction Hamiltonian of eq.(A.6) may be diagonalized in terms of a proper eigenstates (superposition of the eigenstates of the original atomic Hamiltonian H_0) as given below [3].

$$H_{dd} = \begin{pmatrix} \frac{1}{\sqrt{2}} & \frac{}{R^3} & 0 \\ 0 & & \frac{}{R^3} \end{pmatrix} \tag{A.7}$$

for

$$|\ i = \frac{|\ _l i\ |\ _r i}{\sqrt{2}} = \frac{|1_i;0_j i\ \ |0_i;1_j i}{\sqrt{2}}$$

$$= \frac{|1_i i\,|0_j i\ \ |0_i i\,|1_j i}{\sqrt{2}} \tag{A.8}$$

where corresponds each other, all the dipoles are assumed to be along an axis (ex. z), is a constant, and $R = jR_i \quad R_j j$. The digenerated energy level causes splitting by an amount $E_{dd} = \frac{2}{R^3}$, as represented in Fig.A1.

For an ensemble of w dipole pairs in N quantum dots, the collection of the energy splittings amounts to the total energy splitting $w\frac{2}{R^3}$, which may corresponds to the localized mode coherently induced throughout the ensemble, as predicted elsewhere [1] by the quantum mechanical derivation, including coherent state representation, path integral, Lagrangian dynamics, and Green function analysis.

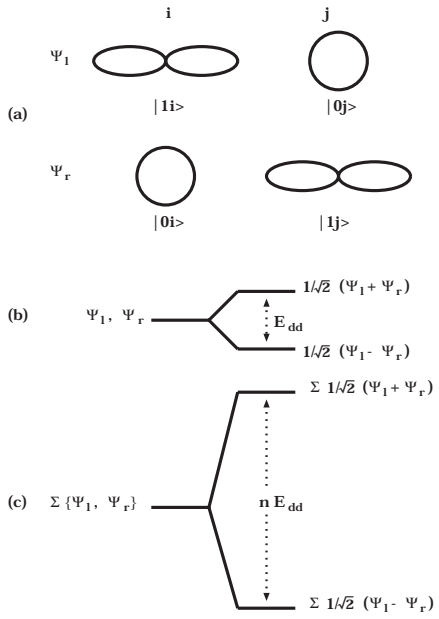

Figure 5: Energy levels generated by the dynamic dipole-dipole interaction among the quantum dot ensemble. (a) degenerate combinations $_l$ and $_r$ of s-like and p-like wave functions at sites i and j, (b) energy splitting E_{dd} due to a pairwise dynamic dipole-dipole interaction, (c) collection of the pairwise dynamic dipole-dipole interaction energy for a w pair ensemble w E_{dd}.